RSC Advances

ROYAL SOCIETY OF CHEMISTRY

www.rsc.org/advances

Journal Name RSC Advances Dynamic Article Links►

Cite this: DOI: 10.1039/c0xx00000x

www.rsc.org/xxxxxx

ARTICLE TYPE

HF-assist one-step synthesis of pompon-like/chip-like $FeSe_2$ particles and their superamphiphobic/antireflective property

Jing Yu,[a] Huijie Wang,[a] NaiqiangYin,[a] and Xiaoliang Xu*[a]

Received (in XXX, XXX) Xth XXXXXXXXX 20XX, Accepted Xth XXXXXXXXX 20XX
DOI: 10.1039/b000000x

Hydrofluoric acid (HF)-assist one-step synthesis of pompon-like/chip-like $FeSe_2$ particles by a solvothermal method has been studied in this paper for the first time. By adjusting the dosage of HF used, $FeSe_2$ particles with pompon-like and chip-like morphologies were obtained. Reaction mechanism was presented based on the experimental phenomena and clearly explained the roles HF played in the synthesis, proving that HF had great influence on controlling the morphologies of $FeSe_2$ particles. By altering the iron sources without any other conditions changed (similar experimental results were observed) we further demonstrated this method was universal. Wettability and lights-trapping effects of the pompon-like/chip-like particles were researched respectively. After modified with heptadecafluorodecyltrimethoxy-silane (HTMS), pompon-like particles exhibited excellent superhydrophobic/surperoleophobic (superamphiphobic) property with water/oil contact angle about 156.0 °/154.6 ° and water/oil sliding angle about 2.0 °/5.0 ° respectively, and ultralow reflectance of the samples (lower than 3 %) in the whole wavelength range of 300 nm-1800 nm were also found in our experiments. Utilizing HF to control the morphologies of $FeSe_2$ particles is an innovative attempt and will show promising potential in controlling morphologies of other transition metal chalcogenides.

Introduction

In recent years, transition metal chalcogenides have sparked worldwide interests to researchers owing to their tunable optical, electrical and magnetic properties.[1-8] Among these chalcogenides, iron selenide ($FeSe_2$), as a p-type chalcogenides semiconductor, has striking application prospects in solar energy fields on account of its narrow band gap energy (E_g=1.0 eV) and high optical absorption coefficient.[1, 9-11] There are lots of ways to synthesize $FeSe_2$, including hydrothermal synthesis,[12] solvothermal synthesis,[1, 9, 13] soft selenization of iron films,[14, 15]electrodeposited method[11], etc. $FeSe_2$ synthesized by different ways has diverse morphologies and sizes, which play important roles in their physical properties.[9, 11, 12] Although some unique morphological $FeSe_2$ have been reported and found with well physical properties, it's far from enough for researchers to understand and make use of them. Therefore, we need to seek new methods to synthesize $FeSe_2$ with various morphologies to bring us better physical performances.

Hydrofluoric acid (HF) has been proved to be effective in changing the morphology of ZnO in Yang's research with little dosage,[16] but if HF can be utilized to control the morphology of $FeSe_2$ is still unknown to researchers. Inspired by this view, we introduced HF in the reaction and successfully synthesized the pompon-like $FeSe_2$ particles by one-step method: heating the mixture of ferrous chloride ($FeCl_2{\cdot}4H_2O$), selenium powder (Se), oleylamine (OLA) and moderate HF at 200 ℃. Then we increased the amount of HF without other experimental conditions changed and found the shape of the $FeSe_2$ started to turn from pompon-like particle to chip-like slices. When excess HF was added, particles finally transformed into the slice. Based on the morphological changes, we proposed a reaction mechanism and legitimately explained the roles HF played in the synthesis, proving that HF had great impact on controlling the morphologies of $FeSe_2$ particles. Then basically same experimental phenomena were found when replacing $FeCl_2{\cdot}4H_2O$ with ferrous sulfate ($FeSO_4{\cdot}7H_2O$), further implying this method was wide-applicable.

Wettability is a very important physical property to surface materials, materials with water/oil contact angle (CA) larger than 150° and sliding angle (SA) less than 10° are usually regarded as superhydrophobic/surperoleophobic (superamphiphobic) materials.[17] Two major factors are required for fine superamphiphobic performance: surface roughness and low surface energy.[18, 19] As a result, there are two ways to obtain superamphiphobic materials: (1) building rough structures by low-surface-energy materials directly[20, 21]; (2) constructing rough structures by other materials and modifying these structures with low-surface-energy chemicals.[16, 22-26] Between the two ways, the latter is more important due to its ability to switch the non-superamphiphobic materials to superamphiphobic materials. This method was also adopted in our experiments by modifying the pompon-like $FeSe_2$ particles with heptadecafluorodecyltrimethoxy-silane (HTMS). After modification, the pompon-like $FeSe_2$ particles possessed

excellent superamphiphobic property with water/oil CA about 156.0 °/154.6 ° and water/oil SA about 2.0 °/5.0 ° respectively, moreover it was also found the superhydrophobic property can maintained well in a wide pH scope (1-14). These properties endowed the particles with well self-cleaning function and corrosion resistance. At last, light-trapping effect of the particles was researched and ultralow reflectance (lower than 3 %) was observed in the wavelength range of 300 nm-1800 nm, guaranteeing the $FeSe_2$ particles sufficient lights absorption.

Our approach is a creative exploration in controlling the morphology of $FeSe_2$ and may be used in the synthesis of other transition metal chalcogenides. What's more, the low price and little dosage of HF make this method economical and efficient in the extensive $FeSe_2$ synthesis in the future.

Experimental

Materials

Selenium powder (Se, AR) was purchased from Shanghai Meixing Chemical Reagent Co., China, oleylamine (OLA, 70%) was purchased from Sigma-Aldrich (USA), and heptadecafluorodecyltrimethoxy-silane (HTMS) was made by Dow Corning Co (USA). Other reagents, including ferrous sulfate ($FeSO_4 \cdot 7H_2O$, AR), ferrous chloride ($FeCl_2 \cdot 4H_2O$, AR), hydrofluoric acid (HF, 40 wt.%, AR), absolute alcohol (AR), hexahydrobenzene (AR), toluene (AR), ethylene glycol (AR), diiodomethane (AR) and formamide (AR), were all obtained from Sinopharm Chemical Reagent Co., Ltd. Cover glasses (22 mm×22 mm×0.15 mm) were obtained from Jiangsu Feizhou Plastic Product Co., China.

Synthesis of $FeSe_2$ particles

Solution 0 was prepared by stirring the mixture of OLA (5 mL), $FeCl_2 \cdot 4H_2O$ (0.0318 g) and Se (0.0505 g), which were held in a vial, for 30min. Preparations of solution 1-4 were almost the same as solution 0, except that different amounts of HF (10 μL, 50 μL, 100 μL, 200 μL) were added into the mixed solution respectively after 30 min stirring, with extra 2 min stirring. All the solutions were heated at 200 ℃ for 1 h with continuous stirring. After the heattreatment, the solutions were cooled to room temperature naturally, the black precipitates were obtained by centrifugation at 8500 rpm for 5 min and refined by washing them with the solution of alcohol/hexahydrobenzene (4/1 vol.) for 5 times. At last, the purified particles dried in vacuum overnight for further characterization. For a better description, these particles were named as sample 0-4, which were corresponding to solution 0-4 respectively.

Surface modification

One third of the every sample was mixed with absolute alcohol (500 μL) respectively to form the rheumy 'coating', these 'coatings' were smeared on the cover glasses (22 mm×22 mm×0.15 mm) uniformly and dried at room temperature. HTMS (150 μL) and toluene (3 ml) were added into a beaker followed by a 1 min ultrasonic treatment to make the solution uniform. The beaker and all the samples were put into a sealedcase, which then was sealed and heated in a drying oven at 90 ℃ for 4 h. After heattreatment, the case was opened in a fume cupboard and the samples were cooled to room temperature naturally.

Characterization

Microstructures of the $FeSe_2$ particles were presented by scanning electron microscopy (SEM) images, which were obtained on a field emission scanning electron microscope (JSM-6700F, 5.0 kV). Transmission electron microscopy (TEM) image and high-resolution transmission electron microscopy (HRTEM) image, which were used to analyse the nanostructure and the crystallization direction of $FeSe_2$ 'petal', were obtained by high-resolution transmission electron microscope (JEM-2011). X-ray diffractive patterns (2θ ranges from 20 °to 70 °) obtained by X-ray diffractometer (TTR-III) were used to analyse the phase, purity and crystallization of the samples. Contact Angle Tester SL200B (Solon Tech (Shang Hai) Co., Ltd.) and its relevant software (CAST 2.0) were used to test the CAs and SAs of the samples with 4.0 μL water/oil droplets on the surfaces of the coated glasses. To investigate the corrosion resistance of the pompon-like particles, water droplets with different pH values were used. All the values of CAs and SAs in this paper were averages, which were obtained by measuring five times at different regions of the surface. Diffuse reflectance spectrums, which could characterize the light-trapping effect of the particles, were given by SolidSpec-3700 UV-VIS-NIR Spectrophotometer (SHIMADZU).

Results and discussion

Crystallization and phase

Fig. 1 presents the XRD patterns of the sample 0-4 in 20 °-70 ° 2θ range. It's observed that all the peaks in patterns correspond well with the standard diffraction peaks (PDF#65-1455), indicating that all samples are orthorhombic iron selenide. What's more, without impurity peaks (such as FeSe, $FeCl_2$ or Se) being observed, XRD patterns demonstrate the high purity and crystallization of the particles.

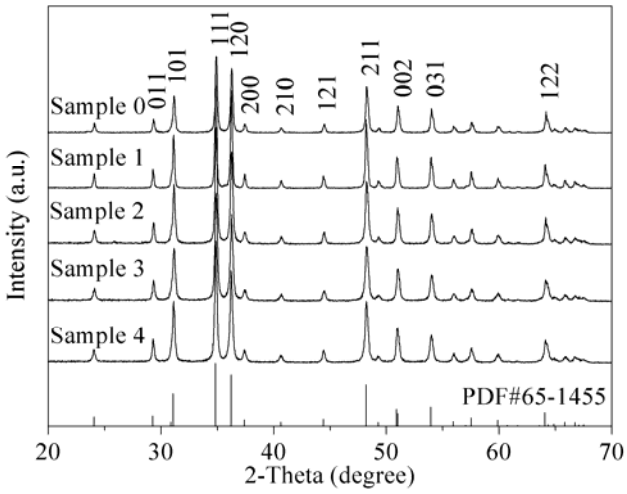

Fig. 1 XRD patterns of $FeSe_2$ particles (sample 0-4).

Morphologies and growth mechanism

Fig. 2 (a) and (b) exhibit the SEM images of sample 0 and sample 1 respectively, insets in the bottom left corners are the corresponding magnified images. It's observed that sample 0 shows a bush-like lumpish structure with the branches diameters

ranging from 60 nm to 110 nm and lengths ranging from 200 nm to 400 nm, while sample 1 shows a regular pompon-like spherical structure with average sphere diameter 1.56 μm. By comparing sample 0 with sample 1, it's found that on one hand the dispersive 'pompons' are obviously smaller than the bush-like chunks, and on the other hand the rod-like 'petals' of sample 1, whose lengths ranging from 164 nm to 251 nm and widths ranging from 119 nm to 234 nm, are shorter and wider than those of sample 0. In consideration of other experimental conditions are unchanged except for the use of HF, it's reasonable to speculate that HF plays a great role in formation of the $FeSe_2$ particles. To clearly understand this influence mechanism, we altered the HF dosage without other conditions changed and observed the morphological changes of $FeSe_2$ to research the relationship between them.

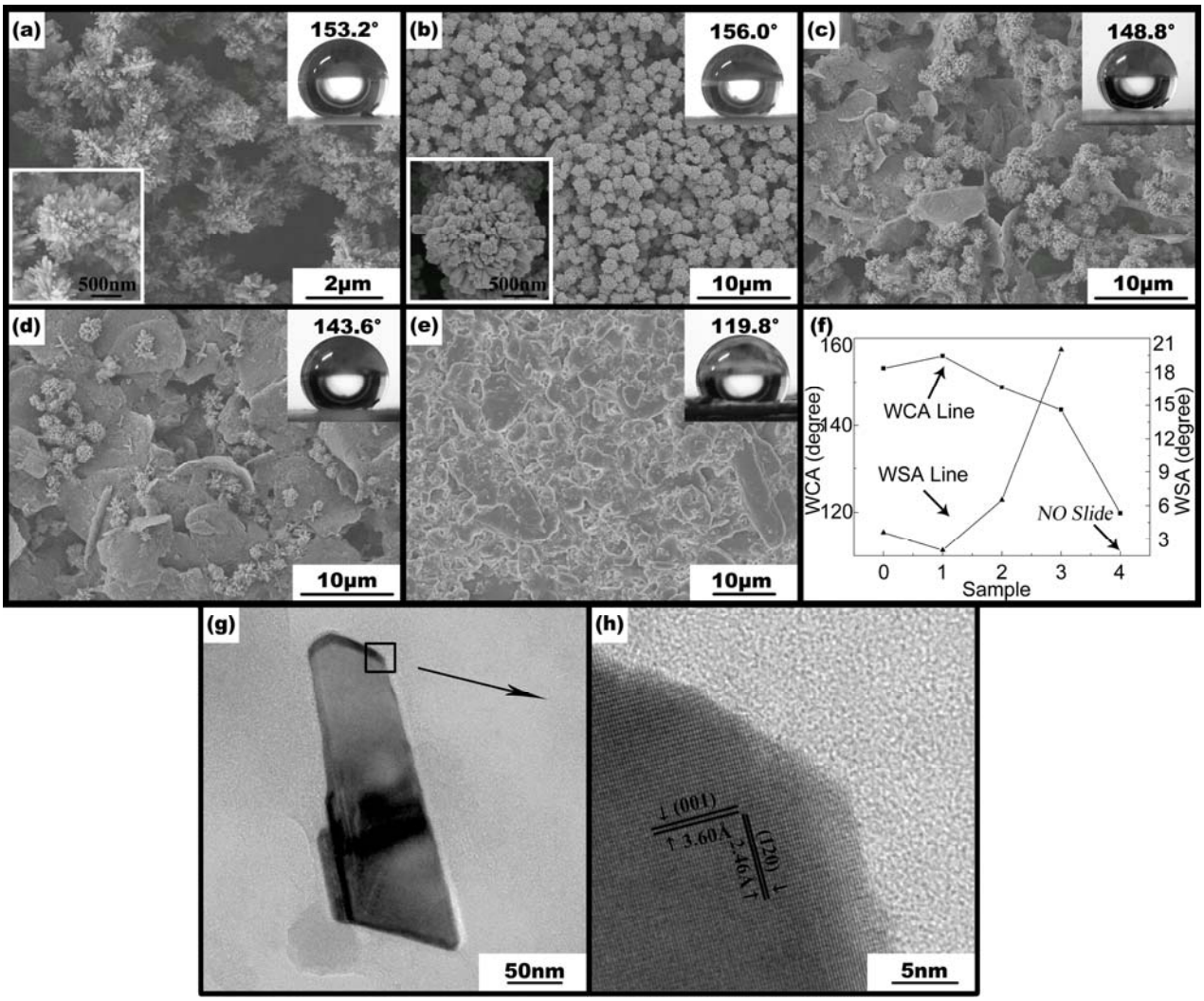

Fig. 2 (a)-(e) are the SEM images of sample 0-4 respectively, insets in the bottom left corners of (a) and (b) are the corresponding magnified images, insets in the top right corners of (a)-(e) are the corresponding water CA images where the droplets are all 4.0 μL with pH=7, (f) is the water CA and SA variation diagram of different samples, (g) is the TEM image of $FeSe_2$ 'petal' stripped from sample 1, (h) is the corresponding HRTEM image of (g).

Fig. 2 (c)-(e) show the morphological variations of $FeSe_2$ particles when different amounts of HF are used: (c)-(e) correspond to sample 2-4 respectively, where the HF dosages are 50 μL, 100 μL and 200 μL respectively. In Fig. 2 (b) well dispersive 'pompons' are the main existing forms without any morphologies being observed, but in Fig. 2 (c) when 50 μL HF is used chips begin to appear. Increasing the amount of HF to 100 μL, numbers of 'pompons' decrease obviously in contrast with sample 2 and chips occupy most part of the $FeSe_2$. Finally, when HF is increased to 200 μL stacked chips turn into the dominating morphology. Combining these morphological variations with those results obtained from Fig. 2 (a) and (b), we have every reason to believe that the HF plays an important role in the synthesis of $FeSe_2$ particles. Fig. 2 (g) and (h) are the TEM and corresponding HRTEM images of $FeSe_2$ 'petal' stripped from sample 1. The 'petal' in (g) shows same size as observed in (b). Clear lattice points are observed in the HRTEM image, intimating the excellent crystallization of the $FeSe_2$ particles which corresponds well with the results obtained from XRD pattern above. Two kinds of mutually perpendicular fringes can be observed, where the plane intervals of different fringes are 3.60 Å and 2.46 Å respectively. Combining with the values provided by Powder Diffraction File (PDF#65-1455), it's reasonable to consider that the two fringes correspond to (001) (3.58 Å) and

(120) (2.48 Å) lattice plane respectively. To further explain these results, we propose the following suppositions:

We think that at the beginning of the reaction $FeSe_2$ seed crystals are formed as the original existing form in solution. Then these seed crystals will experience two synchronous processes: (1) growth of the seed crystals; (2) self-assembly among different seed crystals. Process (1) makes the seed crystals grow to nanorods and process (2) makes these nanorods form bush-like structures. One thing to realize is that without HF in solution process (2) is dominated compared with process (1), which can be confirmed in Fig. 2 (a) where the bush-like lumpish structure formed through process (2) is the main morphology and the rod-like 'petals' formed through process (1) is the subordinate morphology. When HF is added, the seed crystals will adsorb some F^- ions on their surfaces, which will both restrain the growth and the self-assembly of the seed crystals. Affected by this suppression, the size of sample 1 is smaller than that of sample 0. What's more, on the basis of the fact that 'petals' of sample 1 are shorter and wider compared with sample 0, we infer that the radial growth is restrained more than the transverse growth. When the dosage of HF is increased, restraint effects enhance, moreover the restraint to process (1) is weaker than process (2), so finally this restraint leads to two results: one is that the seed crystals will grow alone rather than aggregate together, and another is that the seed crystals will grow to 'chips' due to radial-growth restrain. So, when 200 μL HF is used, there are no 'pompons' in sample 4 except for the stacked 'chips'.

Fig. 3 simply demonstrates the growth mechanism of $FeSe_2$ particles discuss above.

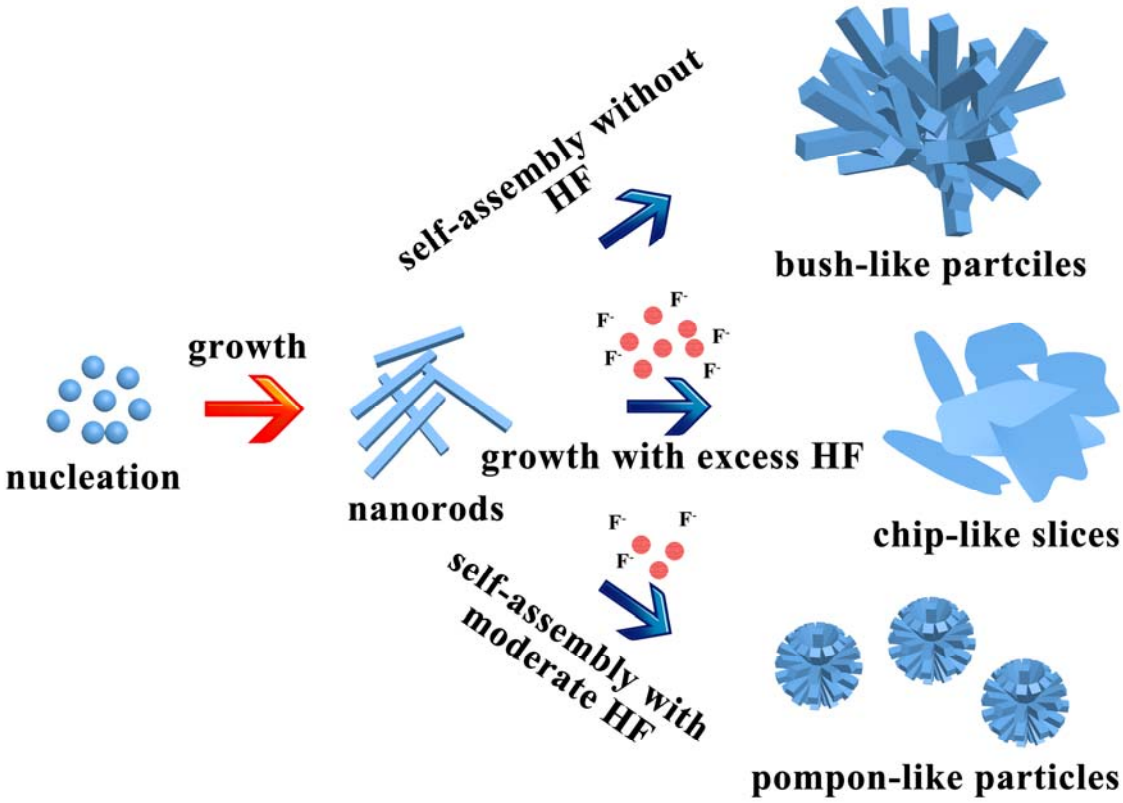

Fig. 3 The schematic illustration of the morphological change with dosage of HF.

For further checking our results, we replaced $FeCl_2 \cdot 4H_2O$ by $FeSO_4 \cdot 7H_2O$ without other conditions (molar ratio of Fe to Se 4:1) changed except that the temperature rose to 220 ℃. Fig. 4 exhibits the morphological variations of $FeSe_2$ particles synthesized by $FeSO_4 \cdot 7H_2O$: (a)-(d) are the $FeSe_2$ particles synthesized with 0 μL, 10 μL, 50 μL and 200 μL HF respectively. In Fig. 4, basically same phenomena like in Fig. 3 are observed: moderate HF (10 μL) helps the $FeSe_2$ particles to form more regular pompon-like particles and excess HF (50 μL or 200 μL) makes the structure change from 'pompons' to 'chips'. An interesting thing is that the 'pompons' formed by $FeSO_4 \cdot 7H_2O$ (average sphere diameter is 670 nm) are smaller than those formed by $FeCl_2 \cdot 4H_2O$ by comparing Fig. 3 (a) with Fig. 4 (b). We think this is mainly caused by the different iron sources, which are also influential in the formation of $FeSe_2$ particles.[1] Discrepancy between the Fig. 2 (a) and Fig. 4 (a) also reflects this guess to a certain extent.

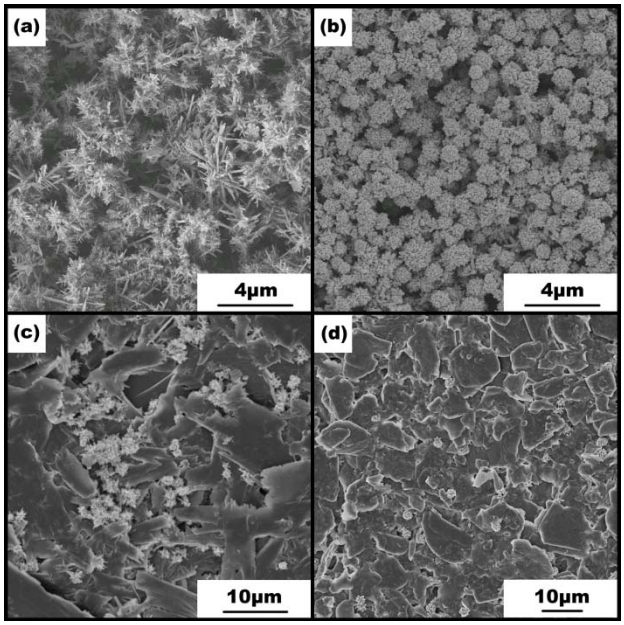

Fig. 4 SEM images of $FeSe_2$ particles synthesized by $FeSO_4 \cdot 7H_2O$ with different amounts of HF: (a) 0 μL, (b) 10 μL, (c) 50 μL, (d) 200 μL.

So far, from the review of experimental results we have just provided, it's reasonable to conclude that adjusting the amount of HF in the reaction can control the morphologies of the $FeSe_2$.

Wettability

Wettability is a very important property for materials, which is closely related to morphologies of materials and has lots of applications, for examples in surface protection. So, wettability of the $FeSe_2$ particles was researched in this paper.

Firstly, we tested the water CAs and SAs of sample 0-4 after modified with HTMS. Insets in the top right corners of Fig. 2 (a)-(e) are the corresponding water CA images of the five samples, CA and SA variations are shown as Fig .2 (f) and snapshot photographs of water droplets rolling off on slant surfaces of samples 0-1 are exhibited in Fig. 5. The water droplets here are all 4.0 μL with pH=7 and the measured values are all averages which were tested at five different points on the same sample. From these data, it's observed that both sample 0 and sample 1 are superhydrophobic, and between them the latter one has larger CA (156.0 °) and less SA (2.0 °) than the former (153.2 °, 3.6 °), implying $FeSe_2$ particles synthesized with moderate HF are better superhydrophobic. But when more HF is added (50 μL, 100 μL, 200 μL), the CA/SA increases/decreases obviously, indicating excess HF destroy the superhydrophobic property of $FeSe_2$ particles.

These CA and SA variations can be ascribed to the morphology changes of $FeSe_2$ particles. As we described former, when moderate HF is used, $FeSe_2$ particles change from bush-like chunk to regular pompon-like particles, which possess better micro-nano structure and therefore are more beneficial to the superhydrophobic property.[27-30] However, when more HF is added, transformation from 'pompons' to 'chips' occurs, resulting in micro-nano structure transforming into micro structure and reducing the surface roughness of the particles. According to the liquid contact theory, this alteration makes liquid-surface contact model change from Cassie model to Wenzel model. Lots of studies have shown that the former model is more excellent than the latter one on superhydrophobic performance, and therefore the CA/SA shows a decrease/increase trend with the increase of HF amount.

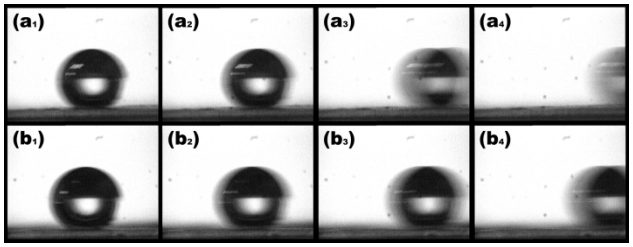

Fig. 5 Snapshot photographs of water droplets (4.0 μL, pH=7) rolling off on slant surfaces of different samples: (a_1)-(a_4) are sample 0, (b_1)-(b_4) are sample 1. Subscript (1)-(4) stand for different shooting times: (1) 0 s, (2) 0.042 s, (3) 0.084 s, (4) 0.126 s.

Secondly, we researched the role that superhydrophobic property of the particles plays in corrosion resistance by altering the pH values of the water droplets then comparing the changes of CA and SA. Sample 1 was chosen as the experimental object on account of its excellent superhydrophobic property. As results shown in Fig. 6, it's observed that although acidity or alkalinity of the water droplets are altered, water CAs/SAs of sample 1 are almost unchanged except for some slight float which can be considered as a normal phenomenon. This is a very important property for our pompon-like particles, because it will ensure their superhydrophobicity in a large pH scope, which makes the sample capable of coping with various extreme difficult conditions for their corrosion resistance.

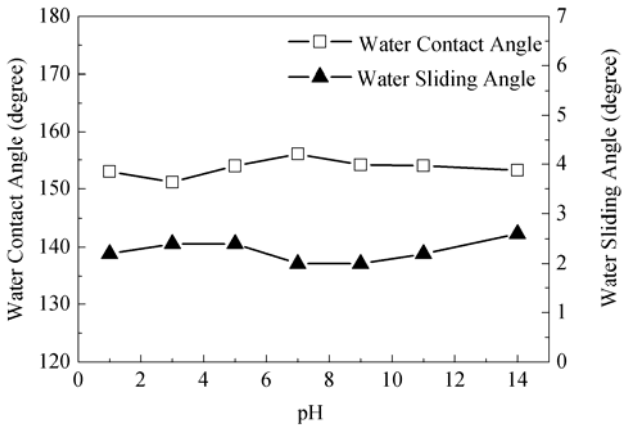

Fig. 6 Water CAs and SAs variations of sample 1 with different pH values.

Thirdly, surperoleophobic property of the particles was investigated, where sample 1 was also chosen as the experimental object. Three kinds of oil, including ethylene glycol, diiodomethane and formamide, were used in this test for research the universality of the surperoleophobic property. Fig. 7 exhibits different oil CAs and SAs of sample 1, and insets in it are the corresponding oil CA images. From this figure, it's found that the $FeSe_2$ particles can always keep oil CAs larger than 150.0 ° and SAs less than 10 °for these three kinds of oil droplets, implying that the modified particles are well surperoleophobic to some extent. Comparing theses data with the water CA and SA (pH=7) of sample 1, it's found that the surperoleophobic property is

slightly worse than the superhydrophobic property, this difference is mainly caused by the lower surface energy of the oil in contrast with water.

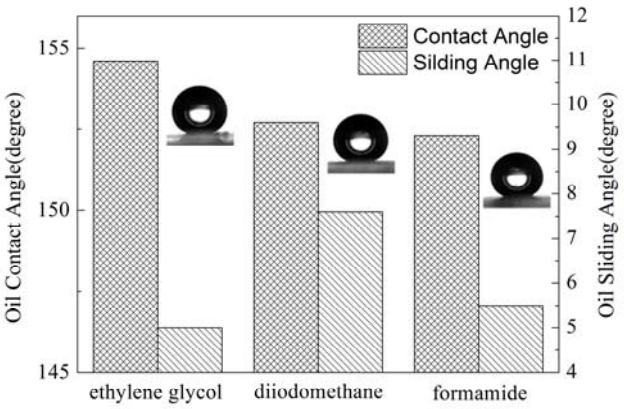

Fig. 7 Oil CAs and SAs of sample 1 with different kinds of oils.

Time-stability of superhydrophobicity of sample 1 was also researched in this paper, and the results are shown in Fig. 8. The water CAs and SAs were measured every month, and it's observed that the CAs and SAs will slightly decrease and increase respectively as time passed in the last year except for some narrow floats at individual data points. This performance indicates that the superhydrophobicity of our particles will decrease when they experience a long-term storage, which may be caused by the slight degeneration of HTMS when it exposed in air for a long time. However, for the worst superhydrophobicity (measured at the twelfth month), the water CA and SA are still in the superhydrophobic scope (water CA: 154.0 °, water SA: 3.7 °). What's more, comparing the worst water CA/SA with the best one, it's found that the difference between them is very small. So, it's still reasonable to believe that our superhydrophobic particles possess a good time-stability.

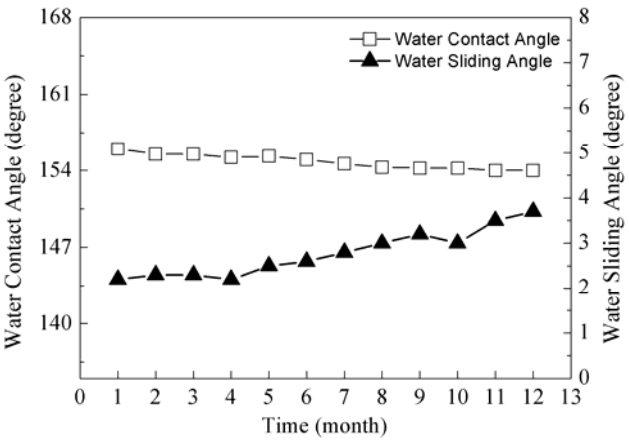

Fig. 8 Water CAs and SAs variations of sample 1 over one year.

Light-trapping effect

At last, we researched the light-trapping effect on the consideration that $FeSe_2$ would be used in the fields of solar cells. Diffuse reflectance of different samples is shown as Fig. 9 (a), where we can observe that all samples possess low reflectance. Among these samples, the reflectance of sample 0-1 are significantly lower in contrast with other samples, and the reflectance of sample 2-4 gradually rise with increase of the amount of HF. The appearance of 'chips' makes the surface flat, which is beneficial to reflect lights, so from sample 2 to sample 4 the reflectance rises in sequence due to the increased numbers of 'chips'. Compared with the relatively flat structures of sample 2-4, low reflectance of sample 0-1 can be ascribed to their rough structures (bush-like structure and pompon-like structure), which can lead incident lights to reflect repeatedly between different particles or between different 'petals' on one particle. Fig. 9 (b) and (c) describe the two different reflection schematics.

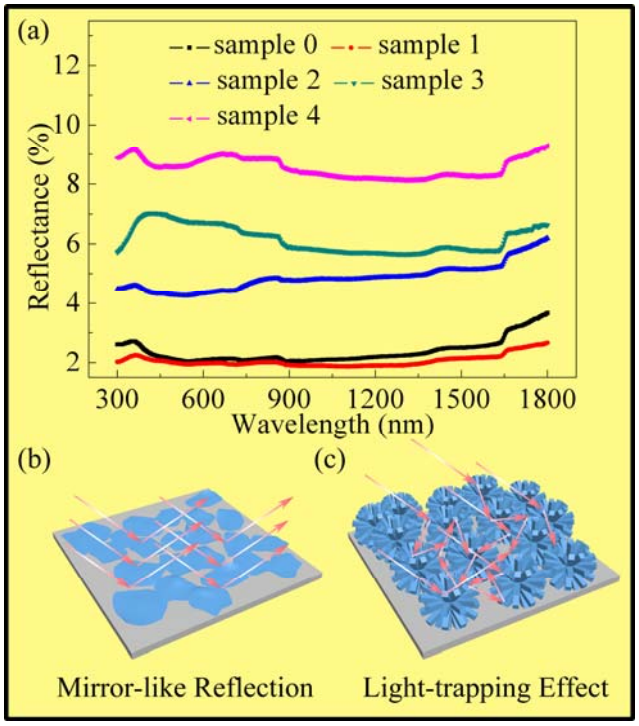

Fig. 9 (a) diffuse reflectance of different samples with wavelength ranging from 300 nm to1800 nm. (b) and (c) two different reflection schematics of $FeSe_2$.

Conclusions

In summary, we utilized HF to successfully synthesize pompon-like and chip-like $FeSe_2$ particles for the first time. We proposed a reaction mechanism of HF and demonstrated HF had significant impact on controlling morphology of $FeSe_2$ particles. Moreover, we further proved this method was suitable for other iron sources by replacing $FeCl_2{\cdot}4H_2O$ with $FeSO_4{\cdot}7H_2O$. For physical performances, wettability and light-trapping effect of the $FeSe_2$ particles were tested. After modified with HTMS, the pompon-like $FeSe_2$ particles were proved to be not only superhydrophobic but also surperoleophobic. Excellent antireflection in the wavelength range of 300 nm to 1800 nm were also found on these pompon-like particles, guaranteeing the particles sufficient light absorptions in application related to solar cells. Our approach is a creative attempt and will show promising potential for controlling morphologies of other transition metal chalcogenides.

Acknowledgements

We sincerely thank the National Natural Science Foundation of China (No. 51272246) and Scientific and Technological Research Foundation of Anhui (No. 12010202035) for financial support.

Notes and references

[a] *Department of Physics, University of Science and Technology of China, Jinzhai Road 96, Hefei, Anhui 230026, P.R. China. Tel: +8655163607574; E-mail: xlxu@ustc.edu.cn*

1. B. X. Yuan, W. L. Luan and S. T. Tu, *Dalton T*, 2012, **41**, 772-776.
2. K. B. Tang, Y. T. Qian, J. H. Zeng and X. G. Yang, *Advanced Materials*, 2003, **15**, 448-450.
3. J. Park, K. J. An, Y. S. Hwang, J. G. Park, H. J. Noh, J. Y. Kim, J. H. Park, N. M. Hwang and T. Hyeon, *Nat. Mater.*, 2004, **3**, 891-895.
4. M. Akhtar, J. Akhtar, M. A. Malik, F. Tuna, M. Helliwell and P. O'Brien, *J Mater Chem*, 2012, **22**, 14970-14975.
5. T. Harada, *J Phys Soc Jpn*, 1998, **67**, 1352-1358.
6. S. Thanikilkarasan, T. Mahalingam, K. Sundaram, A. Kathalingam, Y. D. Kim and T. Kim, *Vacuum*, 2009, **83**, 1066-1072.
7. A. Kathalingam, T. Mahalingam and C. Sanjeeviraja, *Mater Chem Phys*, 2007, **106**, 215-221.
8. H. H. Chen, R. J. Zou, N. Wang, H. H. Chen, Z. Y. Zhang, Y. G. Sun, L. Yu, Q. W. Tian, Z. G. Chen and J. Q. Hu, *J Mater Chem*, 2011, **21**, 3053-3059.
9. J. Xu, K. Jang, J. Lee, H. J. Kim, J. Jeong, J. G. Park and S. U. Son, *Cryst Growth Des*, 2011, **11**, 2707-2710.
10. H. J. Kwon, S. Thanikaikarasan, T. Mahalingam, K. H. Park, C. Sanjeeviraja and Y. D. Kim, *J. Mater. Sci.-Mater. Electron.*, 2008, **19**, 1086-1091.
11. T. Mahalingam, S. Thanikaikarasan, R. Chandramohan, M. Raja, C. Sanjeeviraja, J. H. Kim and Y. D. Kim, *Mater Chem Phys*, 2007, **106**, 369-374.
12. A. P. Liu, X. Y. Chen, Z. J. Zhang, Y. Jiang and C. W. Shi, *Solid State Commun*, 2006, **138**, 538-541.
13. J. Yang, G. H. Cheng, J. H. Zeng, S. H. Yu, X. M. Liu and Y. T. Qian, *Chem Mater*, 2001, **13**, 848-853.
14. N. Hamdadou, A. Khelil, M. Morsli and J. C. Bernade, *Vacuum*, 2005, **77**, 151-156.
15. B. Ouertani, J. Ouerfelli, M. Saadoun, M. Zribi, M. Ben Rabha, B. Bessais and H. Ezzaouia, *Thin Solid Films*, 2006, **511**, 457-462.
16. Z. Yang, X. L. Xu, M. G. Gong, L. Liu and Y. S. Liu, *Chin. Phys. B*, 2010, **19**.
17. K. S. Liu and L. Jiang, *Nanoscale*, 2011, **3**, 825-838.
18. A. Nakajima, K. Hashimoto, T. Watanabe, K. Takai, G. Yamauchi and A. Fujishima, *Langmuir*, 2000, **16**, 7044-7047.
19. W. Ming, D. Wu, R. van Benthem and G. de With, *Nano Lett.*, 2005, **5**, 2298-2301.
20. Y. Zhang, S. Wei, F. Liu, Y. Du, S. Liu, Y. Ji, T. Yokoi, T. Tatsumi and F.-S. Xiao, *Nano Today*, 2009, **4**, 135-142.
21. D. Nystrom, J. Lindqvist, E. Ostmark, A. Hult and E. Malmstrom, *Chem. Commun.*, 2006, 3594-3596.
22. M. G. Gong, X. L. Xu, Z. Yang, Y. Y. Liu, H. F. Lv and L. Lv, *Nanotechnology*, 2009, **20**.
23. Z. W. Wang, Q. Li, Z. X. She, F. N. Chen and L. Q. Li, *J Mater Chem*, 2012, **22**, 4097-4105.
24. D. Z. Xu, M. Z. Wang, X. W. Ge, M. H. W. Lam and X. P. Ge, *J Mater Chem*, 2012, **22**, 5784-5791.
25. M. Wang, C. Chen, J. P. Ma and J. Xu, *J Mater Chem*, 2011, **21**, 6962-6967.
26. C. Chen, J. Xu, Q. H. Zhang, Y. F. Ma, L. P. Zhou and M. Wang, *Chem. Commun.*, 2011, **47**, 1336-1338.
27. Y. B. Zhang, Y. Chen, L. Shi, J. Li and Z. G. Guo, *J Mater Chem*, 2012, **22**, 799-815.
28. L. Feng, S. H. Li, Y. S. Li, H. J. Li, L. J. Zhang, J. Zhai, Y. L. Song, B. Q. Liu, L. Jiang and D. B. Zhu, *Advanced Materials*, 2002, **14**, 1857-1860.
29. Z. G. Guo, F. B. Han, L. B. Wang and W. M. Liu, *Thin Solid Films*, 2007, **515**, 7190-7194.
30. Z. G. Guo, F. Zhou, J. C. Hao and W. M. Liu, *J. Am. Chem. Soc.*, 2005, **127**, 15670-15671.

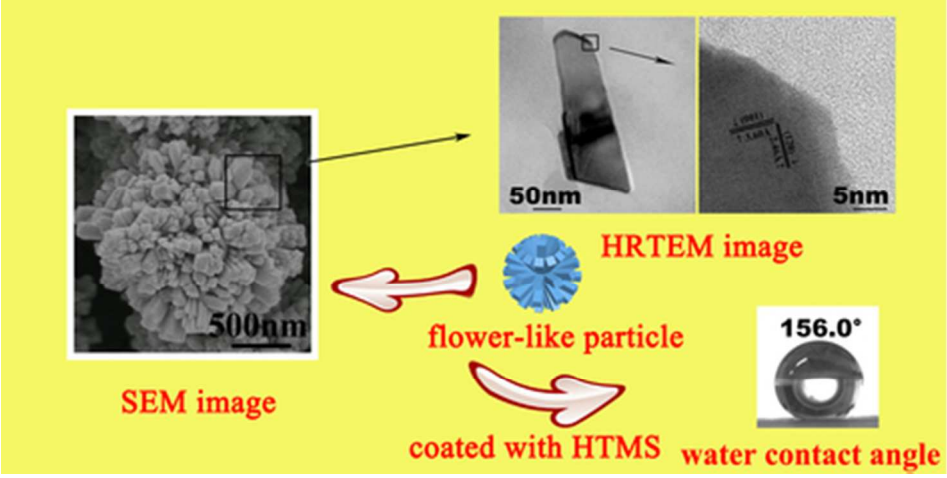

39x19mm (300 x 300 DPI)

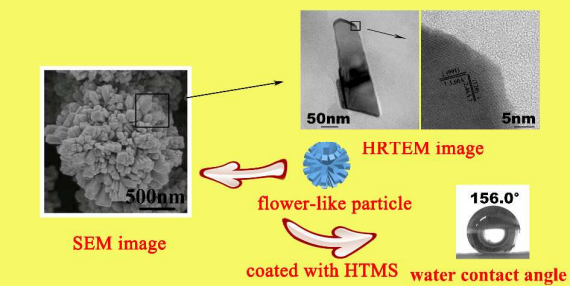

This paper describes a method of controlling the shape of $FeSe_2$ particles with assist of HF